archaeometry

Archaeometry **55**, 2 (2013) 214–234 doi: 10.1111/j.1475-4754.2012.00702.x

ISOTOPES ON THE BEACH, PART 1: STRONTIUM ISOTOPE RATIOS AS A PROVENANCE INDICATOR FOR LIME RAW MATERIALS USED IN ROMAN GLASS-MAKING*

D. BREMS,[1]† M. GANIO,[1] K. LATRUWE,[2] L. BALCAEN,[2] M. CARREMANS,[1] D. GIMENO,[3] A. SILVESTRI,[4] F. VANHAECKE,[2] P. MUCHEZ[1] and P. DEGRYSE[1]

[1]*Division of Geology, Department of Earth and Environmental Sciences, K.U. Leuven, Celestijnenlaan 200E, B-3001 Leuven, Belgium*

[2]*Department of Analytical Chemistry, Ghent University, Krijgslaan 281—S12, B-9000 Ghent, Belgium*

[3]*Departament de Geoquímica, Petrología i Prospecció Geològica, Facultat de Geologia, Universitat de Barcelona, 08028 Barcelona, Spain*

[4]*Dipartimento di Geoscienze, Università di Padova, Via Gradenigo 6, 35131 Padova, Italy*

The provenancing of *Roman natron glass is one of the most challenging problems in the field of archaeometry. Although the use of Sr and Nd isotope ratios and trace element signatures as an indication of provenance has proven promising, there are still many unknowns. In this study, the influence of the different raw materials on the final Sr isotopic composition of Roman natron glass is examined. It is shown that the* $^{87}Sr/^{86}Sr$ *ratio in natron glass is significantly influenced by the silicate fraction of the sand used and does not always provide a clear indication of the lime source used.*

KEYWORDS: STRONTIUM, ISOTOPES, PROVENANCE STUDIES, ROMAN, NATRON GLASS, RAW MATERIALS, BEACH SAND, WESTERN MEDITERRANEAN

INTRODUCTION

Between the fifth century BC and the ninth century AD, the glass most commonly used in the Mediterranean area and the rest of Europe was soda–lime–silica glass of the natron type. The raw materials that were used to produce this kind of glass consisted of quartz-rich calcareous sand, a source of soda called natron and possibly an additional source of lime. The natron was derived from evaporitic lake deposits rich in sodium carbonates (Shortland 2004; Shortland *et al*. 2006). Glass produced with this kind of soda source typically has low concentrations of potassium and magnesium (Sayre and Smith 1961; Freestone 2006; Wedepohl *et al*. 2011a,b).

Natron glass was produced from its raw materials in large tank furnaces. Examples of these production centres have been identified in Egypt and Syro-Palestine. Although the production of raw glass using sand raw materials from Italy, Gaul and Spain is mentioned by a number of classical authors, such as Pliny the Elder and Strabo, actual glass-making sites remain unknown in the western part of the Mediterranean (see also Silvestri *et al*. 2006; Degryse and Schneider 2008; Freestone 2008; Brems *et al*. 2012a). Without any clear evidence from excavations, much archaeometrical research has been conducted with the aim of determining the provenance of ancient glass, and proving or disproving the existence of a primary Roman glass industry in the western part of the Empire. However, over the past decades it has been shown to be very difficult to link a glass artefact to a particular source or site of production (e.g., Degryse *et al*. 2009). Since

*Received 14 March 2012; accepted 4 June 2012

†Corresponding author: email dieter.brems@ees.kuleuven.be

the major and minor elemental compositions of Roman natron glasses have been found to be relatively uniform (Freestone 2006; Wedepohl *et al*. 2011a,b) and hardly ever diagnostic for their origin, other methods had to be found to provenance ancient glass artefacts. In recent years, the use of trace elements and radiogenic isotopes has been shown to offer great potential. Radiogenic isotopes are often relied upon in earth sciences and sedimentary geology, for a wide range of applications, such as dating the formation of rocks and minerals (geochronology), chemical stratigraphic correlation, and tracing the sources and transport of dissolved and detrital constituents in sedimentary, hydrological and biogeochemical cycles (Banner 2004). In particular, Sr and Nd isotope ratios are powerful tracers for sediments. Because of their relatively large masses and small relative mass differences, the isotopic fractionation of the different isotopes of Sr and Nd is negligible in this context (Stille and Shields 1997; Banner 2004). Therefore, the isotopic composition of these elements in a glass is expected to be identical to that of the raw materials from which it was derived. In this paper, we investigate the influence of the different raw materials used in the production of natron glass on the Sr isotopic signature of the final product. In doing so, we can evaluate the usefulness of Sr isotopic signatures in the provenance determination of Roman natron glass. In a second paper (Brems *et al*. 2012b), we discuss the use of Nd isotopic analysis for the provenancing of Roman glass-making.

THE Rb–Sr ISOTOPIC SYSTEM

Strontium has four naturally occurring stable isotopes. The amounts of the isotopes ^{84}Sr, ^{86}Sr and ^{88}Sr are constant in nature. However, ^{87}Sr is radiogenic as it is the product of beta decay of ^{87}Rb.

Because of the differences in their chemical properties, Sr and Rb behave differently in various geochemical processes. Rb is much more incompatible than Sr and, therefore, it is strongly concentrated in partial melts of the mantle that rise and solidify as crustal rocks (Wedepohl 1978, 1995; Stille and Shields 1997; Banner 2004). This elemental fractionation leads to the formation of a number of geochemically different reservoirs with their own specific Sr/Rb elemental and isotopic properties (Stille and Shields 1997). While the mantle has a relatively uniform and low ^{87}Sr/^{86}Sr ratio, the continental crust has a much more variable and, on average, higher ratio. Old Rb-rich rocks contain much more radiogenic ^{87}Sr than younger rocks. The ^{87}Sr/^{86}Sr ratio of the earth at the time of its formation is estimated to be 0.69908 (Faure and Mensing 2005). Since additional ^{87}Sr has been produced ever since, the Sr isotopic signature of the present-day mantle has increased to 0.704 ± 0.002. Crustal-rock ^{87}Sr/^{86}Sr isotope ratios can vary from approximately 0.703 for young basaltic rocks to 0.750 for granites formed from older continental crust (Graustein 1989; Bentley 2006). This difference in Sr isotopic signatures of different types of rock allows them to be used as a tracer for atmospheric dust and detrital components in sedimentary basins (Stanley *et al*. 2003; Banner 2004; Grousset and Biscaye 2005). Regional variations in ^{87}Sr/^{86}Sr values of sediments are a function of the following features of the source rocks: (1) the mineralogy, age and crustal versus mantle source for igneous and metamorphic rocks; (2) the provenance and maturity for sandstones and shales; and (3) the age and extent of alteration for marine carbonates, evaporites and phosphorites (Wedepohl 1978; Banner 2004). Shifts in the isotopic composition can be caused by weathering, transport and diagenetic processes (Linn and DePaolo 1993).

Another interesting and useful application of the Rb–Sr isotopic system arises from the long residence time of Sr in the oceans. Strontium is present in seawater as a trace element, with a concentration of about 7 mg l^{-1} (Stille and Shields 1997). Because of its long residence time (5×10^6 y) relative to the inter-ocean mixing time (1.5×10^3 y), seawater has a very homogeneous

Sr isotopic composition, with $^{87}Sr/^{86}Sr = 0.709165 \pm 0.000020$ (Stille and Shields 1997; Banner 2004). This value, however, did vary through geological time due to variations in the combined inputs from crustal (high $^{87}Sr/^{86}Sr$ ratios) and mantle (low $^{87}Sr/^{86}Sr$ ratios) sources (Burke *et al*. 1982; Banner 2004). Due to their high absolute mass, mass-dependent fractionation of strontium isotopes during the formation of seashell is very limited and the Sr isotopic composition of unaltered marine limestones is thus a very good approximation for the Sr isotopic signature of seawater at the time the limestones were formed (Burke *et al*. 1982). This seawater Sr isotope curve can be used for stratigraphic correlation and to date marine carbonates (Stille and Shields 1997; Veizer *et al*. 1999; Banner 2004).

THE ORIGIN OF Sr IN ANCIENT NATRON GLASS

The bulk of the strontium in the earth's crust occurs as a trace element, dispersed in rock-forming and accessory minerals. The ionic radius of Sr^{2+} (0.113 nm) is intermediate between those of Ca^{2+} (0.099 nm) and K^+ (0.133 nm) (Shannon 1976). As a consequence, strontium readily substitutes for calcium in minerals, such as aragonite, calcite, plagioclase and apatite. To a lesser extent, strontium can also replace potassium in K-feldspar. To maintain electrical neutrality, this substitution of K^+ by Sr^{2+} must be accompanied by the replacement of Si^{4+} by Al^{3+}. The strontium concentration levels in other common rock-forming silicate minerals are considerably lower than those found in the feldspar, where they can reach up to 5000 ppm (Wedepohl 1978). Because they have the same ionic charge and similar ionic radii (Shannon 1976), Rb^+ (0.148 nm) generally substitutes for K^+ (0.133 nm) in all K-bearing minerals, such as K-feldspar, micas, clay minerals and others. Rb^+ is practically excluded from carbonates, since its ionic radius is too large to occupy the Ca^{2+} sites.

Because of a large difference in distribution coefficients for strontium in the different calcium carbonate minerals, the Sr content of seashells and limestones is controlled by the mineralogy. In equilibrium with seawater, aragonite and calcite contain about 8000 and 1200 ppm Sr, respectively (Kinsman 1969; Katz *et al*. 1972). Intermediate values are due to mixed mineralogy of the specimens (Wedepohl 1978). Since aragonite and high-Mg calcite are metastable, they are transformed into stable low-Mg calcite during diagenesis. During this dissolution–precipitation process, the newly precipitated low-Mg calcite will incorporate less Sr into its crystal lattice than the dissolving metastable phases. As a consequence, older limestones with stabilized mineralogy have Sr concentrations an order of magnitude lower than those in the originally deposited material (around 400 ppm—Kinsman 1969; Katz *et al*. 1972; Veizer 1977; Wedepohl 1978). The loss of strontium can also be accompanied by a change in the $^{87}Sr/^{86}Sr$ isotope ratio. This depends greatly on the extent to which the system was closed and the possible presence of an external source of strontium with a different $^{87}Sr/^{86}Sr$ isotope ratio than seawater (Stille and Shields 1997).

In calcareous sediments, such as the beach sands suited for the production of natron glass, strontium is expected to be mainly contained in the carbonate fractions. The $^{87}Sr/^{86}Sr$ ratios of the carbonate are the same as those of the seawater in which it formed and because of the high Sr content, a small amount of calcium carbonate will usually mask the isotopic signature of the silicate fraction (Wedepohl 1978). Depending on the mineralogy and the amount of carbonate present in the sand, varying influences on the bulk $^{87}Sr/^{86}Sr$ isotope ratios may be attributed to the detrital silicate phases (mainly feldspar or clays). The average Sr concentrations in sands and undifferentiated sandstones are in the 30–400 ppm range (Wedepohl 1978).

Roman natron glass contains between 5 and 10% CaO (Foster and Jackson 2009). The bulk of the Sr in Roman glass is believed to have been incorporated with the lime-bearing material

(Wedepohl and Baumann 2000; Freestone *et al*. 2003). Where the lime was derived from Holocene seashell, the Sr isotopic composition of the glass is similar to that of modern seawater. Where the lime was derived from 'geologically aged' limestone, the Sr isotopic signature reflects that of seawater at the time the limestone was deposited, possibly modified by diagenesis. However, other minerals in the sand, such as feldspar and mica, can also influence the Sr budget of the glass batch (Freestone *et al*. 2003; Degryse *et al*. 2006). The contribution of natron to the Sr content and Sr isotopic signature of glass is negligible (Freestone *et al*. 2003). The Sr content of natron glass is also a useful indicator of the source of lime. Since aragonitic seashell may contain a few thousand ppm Sr and calcitic limestone will only incorporate a few hundred ppm of Sr, a similar difference in Sr concentration can be expected in glass produced with these two different sources of lime (Wedepohl and Baumann 2000; Freestone *et al*. 2003). Natron glass melted using limestone contains less than 200 ppm Sr, while shell fragments can bring 300–600 ppm of Sr to the glass.

OBJECTIVES

As described above, the apparent applicability of the Rb–Sr isotopic system to glass studies lies with the assumption that Sr is incorporated into the glass with the lime source. Because of the difference in Sr isotopic signatures of modern seashell and old limestone, the $^{87}Sr/^{86}Sr$ isotope ratio of the glass could be indicative of the nature of the lime source used. However, other minerals naturally included within the sand raw material can also contribute to the final Sr isotopic signature of the glass. The extent of this influence is not well understood.

In this study, we therefore investigated the variation in $^{87}Sr/^{86}Sr$ ratio of possible sand raw materials and the extent of the influence of Sr coming from the sand source on the final Sr isotopic signature of the resulting glass. Seventy-seven beach sand samples from Spain, France and Italy (Fig. 1) were analysed for their Sr isotopic composition. The suitability of the sands for natron glass production has been previously evaluated by calculating the major and minor elemental compositions of glasses that can be produced from these sands and comparing them to the compositional ranges of Roman imperial natron glass (Brems *et al*. 2012a, in press a).

METHODS

Backshore sediment samples were collected from 77 sandy beaches along the coasts of Spain, France and Italy. The sample locations are shown in Figure 1, and their geographical coordinates are given in Table 1. About 2 kg of sediment sample was collected from the upper 10 cm of sand, representing the contemporaneous sedimentation layer. Bulk Sr concentration of the sands were obtained by inductively coupled plasma – optical emission spectrometry (ICP–OES) analysis, as previously described by Brems *et al*. (2012a).

Prior to Sr isotope ratio measurements, Sr was separated from the sample matrix. Sequential extraction procedures developed by De Muynck *et al*. (2009) were combined and slightly modified. Sr isotope ratios were determined using a Thermo Scientific Neptune multi-collector ICP–MS instrument equipped with a micro-flow PFA-50 Teflon nebulizer, coupled on to a spray chamber consisting of a combination of a cyclonic and a Scott-type spray chamber. The measurements were carried out in static multi-collection mode. During $^{87}Sr/^{86}Sr$ isotope ratio measurements, NIST SRM 987 $SrCO_3$ was used as external standard to correct for instrumental mass discrimination (sample-standard bracketing). Before measurements, the Sr concentration in all samples was matched to that of the standard (200 µg l^{-1} Sr) by dilution with 3% HNO_3. The

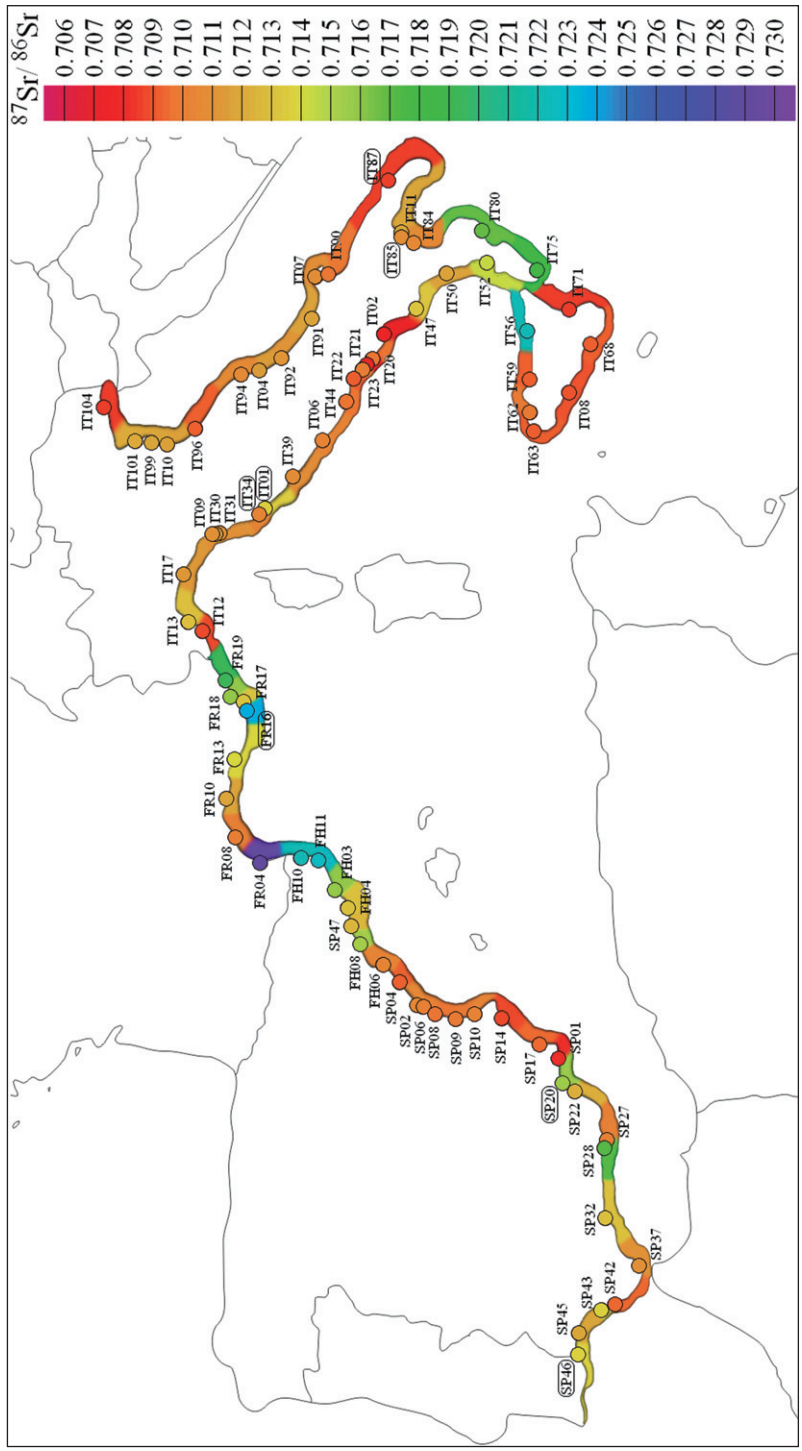

Figure 1 *A map of the western Mediterranean, showing the sample locations and the $^{87}Sr/^{86}Sr$ isotope ratios of the beach sands analysed. Sand samples IT34, IT85 and IT87 have previously been identified as good glass-making sands (*Brems et al. *2012a). Sands SP46, SP20, FR16 and IT01 can be used to make Roman natron glass after the addition of extra lime to the glass batch.*

Table 1 *The sampling locations and results of the Sr isotopic analysis of beach sands from Spain, France and Italy: the Al_2O_3 and CaO data are taken from Brems* et al. *(2012a)*

Sample	*Location*	*Latitude (°N)*	*Longitude (°E)*	*$^{87}Sr/^{86}Sr$*	*2σ*	*Sr (ppm)*	*Al_2O_3 (wt%)*	*CaO (wt%)*	*Al_2O_3/CaO*
Spain									
SP46	Isla Canela	N37°10′34.08″	W007°21′15.58″	0.71378	0.00007	81	3.68	1.59	2.31
SP45	Mazagón	N37°07′44.86″	W006°49′29.42″	0.71197	0.00010	91	1.87	2.09	0.89
SP43	Sanlúcar de Barrameda	N36°46′48.43″	W006°21′59.54″	0.71369	0.00007	76	2.21	2.40	0.92
SP42	El Puerto de Santa Maria	N36°34′40.86″	W006°13′38.77″	0.70949	0.00009	296	1.18	12.11	0.10
SP37	Carteya-Guadarranque (San Roque)	N36°10′51.65″	W005°24′45.42″	0.71089	0.00011	86	1.59	2.56	0.62
SP32	Málaga	N36°43′11.69″	W004°24′14.53″	0.71293	0.00011	133	6.56	6.02	1.09
SP28	Adra	N36°44′38.17″	W003°00′45.75″	0.71716	0.00010	76	5.18	2.19	2.36
SP27	Almerimar	N36°42′07.46″	W002°48′03.33″	0.71018	0.00008	212	3.66	5.94	0.62
SP22	Las Marinas de Vera (Garrucha)	N37°11′50.56″	W001°48′44.82″	0.71222	0.00009	102	3.84	4.87	0.79
SP20	El Rubial	N37°24′02.10″	W001°35′33.26″	0.71559	0.00018	30	2.77	1.24	2.24
SP01	Cartagena	N37°35′	W000°58′	0.70800	0.00007	389	2.15	28.16	0.08
SP17	Mil Palmeras	N37°52′54.13″	W000°45′13.59″	0.70937	0.00009	206	0.78	18.72	0.04
SP14	Villajoyosa	N38°30′23.71″	W000°13′38.11″	0.70885	0.00010	291	0.70	19.16	0.04
SP10	Cullera	N39°09′23.94″	W000°14′24.51″	0.71022	0.00007	186	1.97	17.83	0.11
SP09	Valencia	N39°24′27.55″	W000°19′54.16″	0.70984	0.00010	134	0.99	12.49	0.08
SP08	Sagunto	N39°39′36.15″	W000°12′34.58″	0.70965	0.00010	176	1.99	16.97	0.12
SP06	Castellón de la Plana	N39°59′44.86″	E000°01′43.78″	0.71003	0.00012	230	3.17	19.00	0.17
SP02	Benicassim (Castellon)	N40°02′45″	E000°03′56″	0.71050	0.00007	218	3.02	18.43	0.16
SP04	Benicarló	N40°25′09.84″	E000°26′13.06″	0.70928	0.00009	282	2.16	26.12	0.08
FH06	Riumar	N40°43′49″	E000°50′30″	0.71032		233	3.62	16.15	0.22
FH08	Cambrils	N41°03′57.6″	E001°04′06.3″	0.71520	0.00014	149	7.83	4.90	1.60
SP47	Coma-Ruga	N41°11′00.68″	E001°32′46.71″	0.71253	0.00010	147	5.10	8.41	0.61
FH04	Castelldefels	N41°15′51.7″	E001°57′02.0″	0.71298	0.00014	154	4.99	8.92	0.56
FH03	Vilassar de Mar	N41°30′46.6″	E002°24′46.3″	0.71584		158	11.26	1.72	6.55
FH11	Platja d'Aro	N41°49′02.08″	E003°04′11.10″	0.72264		72	6.67	0.34	19.67
FH10	Sant Pere Pescador	N42°11′21.43″	E003°06′38.18″	0.72232	0.00019	100	8.93	0.68	13.10

Table 1 *(Continued)*

Sample	*Location*	*Latitude (°N)*	*Longitude (°E)*	$^{87}Sr/^{86}Sr$	2σ	*Sr (ppm)*	Al_2O_3 *(wt%)*	*CaO (wt%)*	Al_2O_3/CaO
France									
FR04	Le Barcarès	N42°46′57.21″	E003°02′20.30″	0.72901	0.00019	84	8.90	0.96	9.27
FR08	Le Grau-d'Agde	N43°16′57.91″	E003°26′59.95″	0.71013	0.00013	329	4.75	14.37	0.33
FR10	Saintes-Maries-de-la-Mer	N43°26′57.43″	E004°24′57.79″	0.71177	0.00016	212	5.37	8.69	0.62
FR13	L'Estaque, Plage des Corbières	N43°21′27.36″	E005°17′26.53″	0.71388	0.00019	69	1.77	3.70	0.48
FR16	Les Bormettes, La Londe-les-Maures	N43°07′16.69″	E006°15′38.86″	0.72358	0.00014	50	4.19	0.42	10.04
FR17	Cavalaire-sur-Mer	N43°10′57.28″	E006°32′28.29″	0.71315	0.00013	134	7.70	1.04	7.40
FR18	Saint-Aygulf	N43°24′31.78″	E006°44′06.80″	0.71587	0.00016	143	6.39	9.89	0.65
FR19	Cannes	N43°32′55.72″	E007°00′13.63″	0.71926	0.00026	104	5.32	7.01	0.76
Italy									
IT12	Pigna, Andora SV	N43°56′49.79″	E008°08′27.84″	0.70872	0.00014	545	2.78	14.77	0.19
IT13	Finale Pia, Finale Ligure	N44°10′18.48″	E008°21′30.08″	0.71304	0.00015	75	4.17	6.56	0.64
IT17	Sestri Levante	N44°16′21.51″	E009°23′35.56″	0.71135	0.00015	69	7.39	2.05	3.60
IT09	Torre del Lago Puccini, Viareggio	N43°49′28.23″	E010°15′15.36″	0.71090	0.00007	250	6.55	8.48	0.77
IT30	Migliarino, Vecchiano	N43°47′33.04″	E010°15′55.95″	0.71149	0.00016	206	6.82	6.32	1.08
IT31	Marina di Pisa	N43°40′00.06″	E010°16′30.89″	0.71090	0.00017	259	6.53	8.29	0.79
IT34	Torre del Sale, Piombino	N42°57′14.50″	E010°36′00.71″	0.71034	0.00013	225	2.84	7.99	0.36
IT01	Cala Violina	N42°50′19.53″	E010°46′29.46″	0.71357	0.00002	60	3.12	0.76	4.09
IT39	Montalto Marina	N42°19′41.71″	E011°34′29.44″	0.71073	0.00009	1186	12.56	11.82	1.06
IT06	Ostia	N41°43′41.45″	E012°16′40.78″	0.71033	0.00007	396	5.66	20.49	0.28
IT44	Terracina	N41°16′50.95″	E013°11′47.24″	0.70967	0.00010	482	2.10	17.10	0.12
IT22	Gaeta (BRILL 4556; Degryse and Schneider 2008)	N41°12′47″	E013°32′33″	0.70922	0.00001	169	n.d.	n.d.	n.d.
IT23	Volturno, coastal strip of Mondragone (MN1; Silvestri *et al.* 2006)	N41°07′32.85″	E013°51′55.31″	0.71013	0.00014	377	5.23	20.66	0.25
IT21	Castel Volturno, mouth of Volturno River (BRILL 4554; Degryse and Schneider 2008)	N41°01′15″	E013°55′50″	0.70796	0.00002	423	n.d.	n.d.	n.d.

IT20	Licola Mare (BRILL 4553; Degryse and Schneider 2008)	N40°52′5″	E014°02′37″	0.70969	0.00001	n.d.	n.d.	n.d.	n.d.
IT02	Amalfi	N40°37′07.16″	E014°34′38.54″	0.70748	0.00001	517	7.13	28.05	0.25
IT47	Foce, Marina di Casal Velino	N40°09′41.95″	E015°08′41.66″	0.71326	0.00013	141	6.36	3.04	2.10
IT50	Paola	N39°22′00.36″	E016°01′38.86″	0.71164	0.00011	227	14.82	5.90	2.51
IT52	Pizzo	N38°46′20.22″	E016°11′50.19″	0.71434	0.00009	236	10.23	1.99	5.15
IT56	Scafa, Brolo	N38°09′19.65″	E014°47′57.53″	0.72218	0.00012	97	8.71	1.52	5.73
IT59	San Nicola l'Arena	N38°00′35.31″	E013°37′26.32″	0.70916	0.00013	181	0.71	8.97	0.08
IT62	Castellammare del Golfo	N38°01′28.21″	E012°54′20.29″	0.70990	0.00020	71	0.51	4.71	0.11
IT63	Marausa, Trapani	N37°56′05.62″	E012°28′53.98″	0.70922	0.00010	101	0.38	5.32	0.07
IT08	Torre Salsa	N37°22′12.78″	E013°19′01.45″	0.70895	0.00007	385	0.94	22.12	0.04
IT68	Marina di'Acate	N36°58′58.28″	E014°21′31.86″	0.70914	0.00005	310	1.02	16.70	0.06
IT71	Catania	N37°27′08.69″	E015°05′11.40″	0.70851	0.00015	238	1.39	10.11	0.14
IT75	Bova Marina	N37°55′37.60″	E015°53′24.66″	0.71788	0.00008	199	13.33	1.53	8.72
IT80	Steccato	N38°55′58.25″	E016°55′12.79″	0.71687	0.00013	173	11.62	2.23	5.20
IT84	Lido di Policoro	N40°11′53.62″	E016°43′37.65″	0.71046	0.00016	209	3.44	9.28	0.37
IT85	Metaponto Lido	N40°20′34.11″	E016°49′23.68″	0.71079	0.00054	178	2.67	9.32	0.29
IT11	Castellaneta Marina	N40°27′45.63″	E016°56′18.41″	0.71178	0.00007	203	4.02	11.48	0.35
IT87	Masseria Maime	N40°33′27.00″	E018°02′36.73″	0.70867	0.00012	336	1.26	8.97	0.14
IT90	Siponto, Manfredonia	N41°35′32.58″	E015°53′41.45″	0.70978	0.00014	347	5.95	11.96	0.50
IT07	Gargano	N41°56′11.64″	E015°56′50.84″	0.71088	0.00007	424	4.38	22.82	0.19
IT91	Campomarino	N41°58′39.04″	E015°01′52.56″	0.71163	0.00010	236	4.37	14.44	0.30
IT92	Pescara	N42°28′28.71″	E014°12′40.47″	0.71112	0.00010	287	4.34	22.08	0.20
IT04	San Benedetto del Tronto	N42°57′57.45″	E013°52′48.24″	0.71143	0.00001	199	3.49	16.43	0.21
IT94	Civitanova Marche	N43°17′44.25″	E013°44′30.80″	0.71064	0.00015	181	2.93	18.87	0.16
IT96	Gabicce Mare	N43°58′03.83″	E012°44′25.39″	0.70916	0.00015	589	3.23	29.02	0.11
IT10	Casalborsetti	N44°33′17.84″	E012°17′00.57″	0.71159	0.00007	313	7.64	11.46	0.67
IT99	Lido delle Nazioni	N44°43′54.17″	E012°14′31.82″	0.71192	0.00016	310	7.77	9.71	0.80
IT101	Boccasette	N45°01′37.79″	E012°25′25.92″	0.71202	0.00011	264	9.04	8.10	1.12
IT104	Bibione, Lignano Sabbiadoro	N45°37′53.58″	E013°03′23.80″	0.70846	0.00013	184	1.08	32.46	0.03
Shell	Mixture of shell fragments from southern France and northwestern Italy			0.70915	0.00010	1568	n.d.	n.d.	n.d.

intensities obtained for $^{83}Kr^{+}$ and $^{85}Rb^{+}$ were used to correct for the corresponding contributions at *m*/*z* 84 and 86 (Kr), and *m*/*z* 87 (Rb). On average, $^{87}Sr/^{86}Sr$ isotope ratios were measured with an internal precision (2σ) of 0.0000439.

RESULTS AND DISCUSSION

The results are shown in Table 1 and Figure 1. The beach sands analysed show a wide range of $^{87}Sr/^{86}Sr$ isotope ratios between 0.7075 and 0.7290. The bulk concentration of Sr in the sands varies between 30 and 1186 ppm. In this section, we will discuss the results of the Sr isotopic analysis in relation to the composition and geological provenance of the beach sands. A complete mineralogical description of the sands is beyond the scope of this paper and is presented elsewhere (Brems *et al*. 2012a).

The Iberian Massif and the Betic Cordillera

In southwestern Spain, the Guadiana and Guadalquivir Rivers deliver siliciclastic sediments derived from the crystalline basement of the Iberian Massif to the coast. Beach sands in this region (SP46, SP45 and SP43) contain very small amounts of shell fragments or limestone grains. Therefore, Sr concentrations are rather low (76–91 ppm) and the $^{87}Sr/^{86}Sr$ isotope ratio varies between 0.71197 and 0.71378, indicating the dominant influence of radiogenic Sr from feldspars in the sand. Further south, in the Bay of Cádiz (SP42), sands are derived from Triassic–Cretaceous and Neogene siliciclastic and carbonate sedimentary rocks of the western Subbetic Zone. Here, the beach sand contains about 20% of calcareous fragments from recent seashells and recycled Miocene calcarenites. This additional source of unradiogenic Sr increases the Sr concentration to 296 ppm and lowers the $^{87}Sr/^{86}Sr$ isotope ratio of the sand to 0.70949, which is just above the modern value for seawater.

The Internal Zones of the Betic Cordillera comprise the Malaguide, the Alpujárride and the Nevado–Filábride Complexes and are mostly composed of Palaeozoic metasedimentary rocks. This zone stretches along the southern coast of Spain from Gibraltar to Cartagena. The Sr in all beach sands analysed along this coast (SP37, SP32, SP28, SP27, SP22 and SP20) is provided by two distinct sources. Feldspar and metamorphic rock fragments containing micas and other aluminosilicates are generally present in rather low amounts. However, mixing of these sources of radiogenic Sr with varying amounts of seashell and limestone fragments produces Sr isotopic signatures varying between 0.71018 and 0.71716. Sr contents vary between 30 and 212 ppm. The sands with the highest concentration of calcareous grains show the highest Sr concentrations and lowest $^{87}Sr/^{86}Sr$ isotope ratios, and vice versa. Just east of the city of Cartagena, small pocket beaches alternate with rocky cliffs. Sandy deposits on these small beaches (SP01) are composed of detritus of the local Pliocene dolomitic limestones. This is reflected in the low $^{87}Sr/^{86}Sr$ isotope ratio of this sand, which is 0.70800. The sand contains approximately 65% calcareous fragments. This results in a bulk Sr concentration of 389 ppm.

In the southern part of the Gulf of Alicante, beach sands (SP17) derived from Cenozoic siliciclastic and carbonaceous sedimentary rocks contain 35% calcareous fragments. The $^{87}Sr/^{86}Sr$ isotope ratio of these sands—that is, 0.70937—is just above that of modern seawater, indicating the influence of small amounts of minerals with more radiogenic Sr. North of Alicante and in the southernmost part of the Gulf of Valencia, the erosion of Jurassic to Miocene limestones and sandstones of the Prebetic External Zone of the Betic Cordillera produces sands with abundant

limestone fragments. The Sr budget of the beach sands (SP14) is dominated here by the low $^{87}Sr/^{86}Sr$ isotopic ratios of these limestone grains: 0.70885.

The Iberian System, the Catalonian Coastal Ranges and the Pyrenees

In the eastern part of Spain, Mesozoic and Cenozoic siliciclastic, carbonate and evaporitic sedimentary rocks of the Iberian System overlay the Hercynian basement rocks of the Iberian Massif. The $^{87}Sr/^{86}Sr$ isotope ratios are relatively constant along this part of the Spanish coast. Between Cullera and the Ebro Delta, the beach sands analysed (SP10, SP09, SP08, SP04, SP06 and SP02) all contain quite a lot of calcareous fragments (~20–35%) and small, but significant, amounts of feldspar. The concentration of Sr ranges from 134 to 230 ppm. The $^{87}Sr/^{86}Sr$ isotope ratios are higher than the value for seawater and vary between 0.70965 and 0.71050. Where the sand contains up to 50% calcareous grains derived from Jurassic–Cretaceous limestones (SP04), the Sr content increases to 282 ppm and the $^{87}Sr/^{86}Sr$ isotope ratio is lower and only just above the value for seawater, at 0.70928.

The sediments of the Ebro Delta are derived from the southern flanks of the Pyrenees, the northern side of the Iberian Ranges and the Tertiary sedimentary successions of the Ebro Basin. These sediments (FH06) contain about 30% of calcite, but their $^{87}Sr/^{86}Sr$ isotope ratio of 0.71032 indicates that there must be another source of radiogenic Sr. Between the Ebro Delta and Barcelona, detritus from undeformed Cenozoic and Mesozoic sedimentary rocks is brought to the coast. The combination of about 8–16% calcareous grains and 10% feldspar in beach sand in this area (SP47 and FH04) (Hasendonckx 2009) results in $^{87}Sr/^{86}Sr$ isotope ratios of 0.71253 to 0.71298. Increasing concentrations of feldspar derived from local tonalites and granodiorites in sands near Cambrills (FH08) result in a more radiogenic Sr isotopic signature: 0.71520. The Sr concentrations remain virtually the same (147–154 ppm). North-east of Barcelona, the magmatic bodies of the Catalonian Coastal Ranges are extensively exposed. Similar magmatic rocks occur in the eastern Pyrenees, accompanied by abundant Palaeozoic metamorphic crystalline rocks. Beach sands along the Catalonian Coastal Ranges (FH03 and FH11) and the eastern side of the Pyrenean fold belt in northern Spain and southern France (FH10 and FR04) are practically all lacking carbonate grains. Consequently, the Sr concentrations are rather low (72–158 ppm) and the $^{87}Sr/^{86}Sr$ isotope ratios of these sands are very radiogenic; that is, between 0.71584 and 0.72901.

The Massif Central, the Rhône Basin and the Western Alps

In the central part of the Gulf of Lion, west of the Rhône Delta, beach sands are derived from the weathering products of the southern part of the Massif Central and overlying Jurassic and Cretaceous carbonates and Cenozoic siliciclastic deposits. Bulk $^{87}Sr/^{86}Sr$ isotope ratios for sands in this area (FR08) are a mixture of unradiogenic Sr from carbonate grains and more radiogenic Sr from crystalline basement rocks. This mixing results in a $^{87}Sr/^{86}Sr$ isotope ratio above the modern value for seawater: 0.71013. The concentration of Sr is 329 ppm. Sandy sediments of the Rhône Delta are derived from an extensive drainage area including the Massif Central, the Vosges, the Jura, and the Western and Northern Alps. Although the Rhône sands (FR10) contain about 20% calcareous fragments, the bulk $^{87}Sr/^{86}Sr$ isotope ratio is rather radiogenic, with a value of 0.71177. In the Bay of Marseilles, very mature beach sand occurs between outcrops of Cretaceous and Jurassic limestones. This quartz-rich sand (FR13) is derived from the local

recycling of Oligocene sedimentary rocks. At 0.71388, its $^{87}Sr/^{86}Sr$ isotope ratio is again quite radiogenic due to the scarcity of carbonate grains in the sand, as is also indicated by its low Sr content (69 ppm).

Sands with very radiogenic Sr isotopic signatures are found on the beaches along the metamorphic Maures–Tanneron Massif in south-east France. The highest $^{87}Sr/^{86}Sr$ isotope ratio, 0.72358, occurs near Hyères (FR16), where sediments are derived from the Precambrian metagranites of Bornes, Cambrian quartzites and gneiss, and Ordovician–Silurian schists. These sands contain hardly any calcareous fragments. A bit more to the east (FR17), the isotopic signatures are less extreme, with a $^{87}Sr/^{86}Sr$ ratio of 0.71315. In the Gulf of Fréjus and the Gulf of Napoule, detritus from Cambrian–Ordovician quartzites, schists and granites, and Permian sedimentary and volcanic rocks are mixed with Triassic to Cretaceous limestone fragments. Despite the additional calcareous grains in these sands (FR18 and FR19), the $^{87}Sr/^{86}Sr$ isotope ratios have increased to 0.71587–0.71926. The Sr concentration varies between 104 and 143 ppm.

Sediments derived from Cretaceous to Oligocene calcareous turbidites near Imperia (IT12) have rather low $^{87}Sr/^{86}Sr$ isotope ratios due to the abundance of calcareous fragments in the sand: 0.70872. The high Sr content (545 ppm) indicates the same. In the Gulf of Genoa, Jurassic metaophiolites deliver detritus with very unradiogenic Sr isotopic compositions (Rampone *et al*. 1998) to the beaches. However, because of their very low Sr concentrations, their influence on the Sr budget of the beach sands in this area (IT13 and IT17) is only minor. A mixture of radiogenic Sr from recycled old feldspar and unradiogenic Sr from minor amounts of calcareous fragments results in bulk $^{87}Sr/^{86}Sr$ isotope ratios in the range of 0.71135–0.71304. Sr concentrations remain low (69–75 ppm).

The Tuscan and Roman Magmatic Province

The Arno River delivers sandy sediments to the coastal stretch between Viareggio and Livorno (IT09, IT30 and IT31). These sands are derived from Cretaceous to Oligocene foredeep turbidites and Pliocene–Pleistocene sediments. The $^{87}Sr/^{86}Sr$ isotope ratios of beach sands in this area are relatively similar, at between 0.71090 and 0.71149. The Sr contents lie between 206 and 259 ppm. In the Gulf of Follonica, the beach sands are composed of detritus from turbidite sequences and coastal-plain sediments. These sands are relatively mature, but contain varying amounts of shell fragments (Brems *et al*. 2012a). This has a significant influence on the Sr isotopic signatures and Sr contents of these sands. Beach sand with only trace amounts of calcareous fragments (IT01) shows a rather radiogenic $^{87}Sr/^{86}Sr$ isotope ratio of 0.71357 and low Sr concentrations of 60 ppm. When about 15% of shell is naturally included within the sand (IT34), the Sr concentration is raised to 225 ppm and the $^{87}Sr/^{86}Sr$ isotope ratio is lowered to 0.71034.

Between Monte Argentario and Sperlonga, the Cenozoic potassic volcanic rocks of the Vulsini, Vico, Cimini, Sabatini and Alban Hill volcanoes contribute to the local beach sands (IT39, IT06 and IT44). Also, shell and limestone fragments are present in appreciable amounts in these beach sands and reach concentrations between 15 and 30%. Most of the Sr, however, is present in the volcanic rock fragments containing 500–1500 ppm Sr or even more (Conticelli *et al*. 2002; Avanzinelli *et al*. 2008). This results in very high Sr concentrations in the beach sands, of between 396 and 1186 ppm. $^{87}Sr/^{86}Sr$ isotope ratios of the sands range between 0.70967 and 0.71073. These values are in agreement with those of the volcanic rocks in the area (Di Battistini *et al*. 2001; Conticelli *et al*. 2002; Avanzinelli *et al*. 2008). Further south, the Garigliano and Volturno Rivers bring sediments to the Campanian beaches. These rivers drain an area with abundant volcanic rocks of Roccamonfina and Somma-Vesuvius. The Sr isotopic compositions of

the Volturno sands (IT20, IT21, IT22 and IT23) are influenced by this recent volcanic activity (see also Degryse and Schneider 2008). The sand with the highest concentration of heavy minerals derived from the Pleistocene–Holocene rhyolites (IT21) has the lowest $^{87}Sr/^{86}Sr$ signature—that is, 0.70796—and also the highest Sr content (423 ppm). The other samples contain more shell fragments and recycled feldspars from Miocene turbidites. As a result, their $^{87}Sr/^{86}Sr$ isotope ratios are higher, at 0.70922–0.71013. Sand from a small pocket beach near Amalfi (IT02), south of Vesuvius, is composed of approximately 60% calcareous fragments derived from Triassic–Jurassic–Cretaceous platform carbonates and abundant volcanic detritus. The combination of low $^{87}Sr/^{86}Sr$ ratios from the limestones and unradiogenic Sr derived from the recent volcanic rocks results in a bulk $^{87}Sr/^{86}Sr$ isotope ratio of 0.70748. The Sr concentration of 517 ppm is also rather high.

Jurassic to Oligocene quartzo-feldspathic turbidites along the Cilento promontory are disintegrated into quartz-rich beach sand with substantial amounts of feldspar (IT47). Due to the abundant feldspar and the absence of an important source of calcareous material, the concentration of Sr is low (141 ppm) and the $^{87}Sr/^{86}Sr$ isotope ratio is rather radiogenic (0.71326).

Calabria and Sicily

Calabria and the north-east of Sicily are composed of metamorphic and plutonic rocks of Hercynian age, overlain by syn- to post-Alpine sedimentary cover. The $^{87}Sr/^{86}Sr$ isotope ratios of most beach sands in the Calabria and northeastern Sicily region (IT50, IT52, IT56, IT75 and IT80) are rather high (between 0.71434 and 0.72218) due to the dominance of metamorphic and plutonic rock fragments rich in feldspar and micas. Near Cosenza, on the western coast of Calabria, however, the sands (IT50) contain slightly more calcareous fragments. These carbonate grains, together with small amounts of detritus from local ophiolitic sequences, lower the $^{87}Sr/^{86}Sr$ isotope ratio to 0.71164. Further east along the northern coast of Sicily, in the Termini Imerese Gulf (IT59), quartz-rich beach sands contain about 15% calcareous fragments and only trace amounts of feldspar. Consequently, the $^{87}Sr/^{86}Sr$ isotope ratio of this sand is very close to that of modern seawater, at 0.70916. The Sr concentration is 181 ppm.

In the northwestern part of Sicily, in the Gulf of Castellammare (IT62) and south of Trapani (IT63), sediments are derived from Miocene sedimentary rocks. The combination of traces of feldspar and few calcite grains in these sands results in Sr ratios just above the seawater signature, at 0.70922–0.70990. However, these minerals occur in only very small amounts, resulting in a low Sr content of the sands, at between 71 and 101 ppm. The beach sands along the southwestern part of Sicily (IT08 and IT68) have $^{87}Sr/^{86}Sr$ isotope ratios just below the value for seawater (0.70895–0.70914). In these areas, Sr concentrations are appreciably higher, at 310–385 ppm. In the Gulf of Catania, on the east coast of Sicily, the beach sands (IT71) are mainly derived from Oligocene–Pleistocene sedimentary rocks, with small contributions from volcanic rock fragments from Mount Etna. The $^{87}Sr/^{86}Sr$ isotope ratio of 0.70851 can be explained by the presence of about 20% limestone fragments in the sand and possibly some minor influence from young unradiogenic Mount Etna minerals.

Adria

North of the Calabria region, north-east of the Cape of Spulico, the beach sands are derived from the sedimentary rocks of the Southern Apennines. These sediments (IT84) are delivered to the coast by the Sinni and Agri Rivers. Since feldspar and carbonate fragments make up

about 7 and 20% of the sand, respectively, its $^{87}Sr/^{86}Sr$ isotope ratio lies slightly above the modern seawater signature, at 0.71046. Further north in the Gulf of Taranto, between the mouths of the Basento and the Bradano Rivers (IT85), the $^{87}Sr/^{86}Sr$ isotope ratios remain virtually the same, at 0.71079. Near the city of Taranto (IT11), the sand is a bit richer in feldspar and limestone. The slightly higher $^{87}Sr/^{86}Sr$ isotope ratio (0.71178) indicates that increasing amounts of feldspar have a larger effect on the bulk Sr composition of a sand than additional limestone. On the northeastern coast of Salento, south-east of Brindisi (IT87), the beach sand is composed of detritus derived from the Pliocene–Pleistocene siliciclastic sedimentary rocks overlying the Apulia carbonate platform. Sr seems to be mostly derived from limestone, as is indicated by the low Sr isotopic signature of 0.70867. This is in good agreement with the low feldspar content. However, the sand has a Sr concentration of 336 ppm. This is rather high for a sand with only about 17% limestone grains, and it suggests the presence of some shell material or another source of (unradiogenic) Sr. In the Gulf of Manfredonia (IT90), the sands again contain higher amounts of feldspar from the recycling of immature Pliocene–Pleistocene sedimentary sequences. Consequently, the $^{87}Sr/^{86}Sr$ isotope ratios are above the modern value for seawater, at 0.70978. Along the Gargano promontory (IT07), the combination of abundant limestone fragments and excess feldspar keeps the $^{87}Sr/^{86}Sr$ isotope ratio in the same range (0.71088) and the Sr content relatively high (424 ppm).

The Central Apennines, the Po Basin and the Southern Alps

Between the Gargano promontory and Pesaro (IT91, IT92, IT04 and IT94), the beaches receive their sand from rivers draining the eastern flank of the Central Apennines. These sands are rich in quartz and calcareous fragments, but also contain minor feldspar. The Sr concentrations vary between 181 and 287 ppm. The $^{87}Sr/^{86}Sr$ isotope ratios are relatively uniform and higher than for modern seawater, at 0.71064–0.71163. This indicates the important contribution of radiogenic Sr from the recycled feldspar grains. Between Pesaro and Rimini (IT96), recent shell fragments and detritus from Miocene–Pleistocene limestones make up more than half of the beach sand. Quartz and feldspar occur in lower amounts. Because of this additional source of shell and limestone, the bulk $^{87}Sr/^{86}Sr$ isotope ratio of the sand is lowered to 0.70916 and the Sr content is 589 ppm. Further north, sandy sediments derived from the eastern side of the Northern Apennines are deposited along the beaches near Ravenna (IT10). The $^{87}Sr/^{86}Sr$ isotope ratios of these sands are very similar to those derived from the Central Apennines, at 0.71159.

The drainage basin of the Po River stretches between the Western, Central and Southern Alps and the northwestern side of the Northern Apennines. The combination of 15–20% calcite and ~15% feldspar in the sands along the Po Delta (IT99 and IT101) results in Sr concentrations between 264 and 310 ppm and rather radiogenic $^{87}Sr/^{86}Sr$ isotope ratios of 0.71192–0.71202. The beach sands in the north-east of Italy (IT104) contain very high quantities of calcitic and dolomitic limestone grains (up to 85–90%) and only 10% of silicates. These sediments are the erosion products of the eastern Dolomites and the Carnic to Julian Alps: they have low Sr concentrations (184 ppm) and display a low $^{87}Sr/^{86}Sr$ isotope ratio of 0.70846.

A MIXED Sr ISOTOPE SIGNATURE IN SAND

The large spread in $^{87}Sr/^{86}Sr$ isotope ratios encountered in this study can be attributed to two main sources of strontium. Calcareous fragments in the sand are the first important contributor. Shell fragments occur in widely varying amounts. Sands with large proportions of shell material can

contain high amounts of Sr. Some of the sands analysed are mainly composed of limestone grains. These show lower Sr contents. Shell and limestone fragments deliver Sr with low $^{87}Sr/^{86}Sr$ ratios to the sand. The $^{87}Sr/^{86}Sr$ isotope ratio of the shells is equal to that of present-day seawater; that is, 0.709165 ± 0.000020 (Stille and Shields 1997; Banner 2004). Limestone has even lower $^{87}Sr/^{86}Sr$ isotope ratios, with values depending on the age of the limestone and the extent of diagenesis (Burke *et al*. 1982). The broad range of $^{87}Sr/^{86}Sr$ isotope ratios, with Sr isotopic signatures mostly lying above the modern value for seawater, implies that there must be a second Sr source bringing more radiogenic Sr to the system. The source of this radiogenic Sr must be sought in the silicate fraction of the sand—and most probably in feldspar, and to a lesser extent mica, derived from crystalline magmatic or metamorphic rocks, or recycled immature sedimentary rocks.

The bulk Sr isotopic composition of the sand is a combined signal of the relatively unradiogenic Sr from the carbonates and the higher $^{87}Sr/^{86}Sr$ ratios from the aluminosilicates. This mixed Sr isotopic composition is not only dependent on the absolute content of carbonates and feldspar but also, and even to a much larger extent, on the proportion between the two. This relationship can be seen in Figure 2. Whereas sands containing high CaO values generally have the lowest $^{87}Sr/^{86}Sr$ isotope ratios, these values can still be appreciably higher than the value for seawater (Table 1 and Fig. 2 (a)). The opposite can be seen in the plot of $^{87}Sr/^{86}Sr$ versus Al_2O_3 (Fig. 2 (b)). Sands with low Al_2O_3 concentrations generally have $^{87}Sr/^{86}Sr$ isotope ratios very close to the modern seawater signature. As the Al_2O_3 concentration increases, the range of $^{87}Sr/^{86}Sr$ isotope ratios quickly broadens. The plot of $^{87}Sr/^{86}Sr$ versus Al_2O_3/CaO (Fig. 2 (c)) shows that the $^{87}Sr/^{86}Sr$ isotope ratios of beach sands are only around or below the modern value for seawater, if they contain at least four times as much CaO as Al_2O_3 ($Al_2O_3/CaO < 0.25$). The higher the Al_2O_3/CaO ratio, the higher is the $^{87}Sr/^{86}Sr$ isotope ratio.

In this regional study, only one sand sample was analysed for each beach deposit. Although care was taken to obtain a representative sample, small variations in the ratio of shell fragments to feldspar within the sand deposit cannot be ruled out. These variations would result in small changes in the Sr isotopic signature of the sand. A detailed study with systematic sampling over the stretch of a single beach would be useful, to investigate the possible variation within a single sand deposit.

$^{87}Sr/^{86}Sr$ AS A PROVENANCE INDICATOR OF LIME IN NATRON GLASS?

Roman natron glass generally contains 5–10% CaO (Foster and Jackson 2009). Taking into account the addition of natron and the loss of the volatile fraction during the melting of the glass, this corresponds to about 6–11% CaO in the sand raw material. Sands corresponding to this range of CaO concentrations have varying $^{87}Sr/^{86}Sr$ isotope ratios, between 0.70851 and 0.71926 (Fig. 2 (a)). However, not all of these sands are actually suitable for the production of glass (Brems *et al*. 2012a). Most of them are too elevated in Al_2O_3 and Fe_2O_3, and do not contain enough SiO_2. Only one of the sands analysed (sand IT85 from the south-east of Italy) would, after fluxing it with pure natron, produce a glass with a major and minor elemental composition very similar to that of typical Roman natron glass. Two other sands can be melted into a glass resembling Roman glass for all but one element. Glass made with sand IT34 would have a low P_2O_5 concentration and glass melted with sand IT87 would be unusually low in Al_2O_3 (Brems *et al*. 2012a). The necessary amount of CaO in sands IT85 and IT87 is derived from limestones and marls in the local hinterland. The available CaO in sand IT34 is mostly contained in shell fragments that are naturally included in the sand (Brems *et al*. 2012a). Therefore, we would expect the Sr

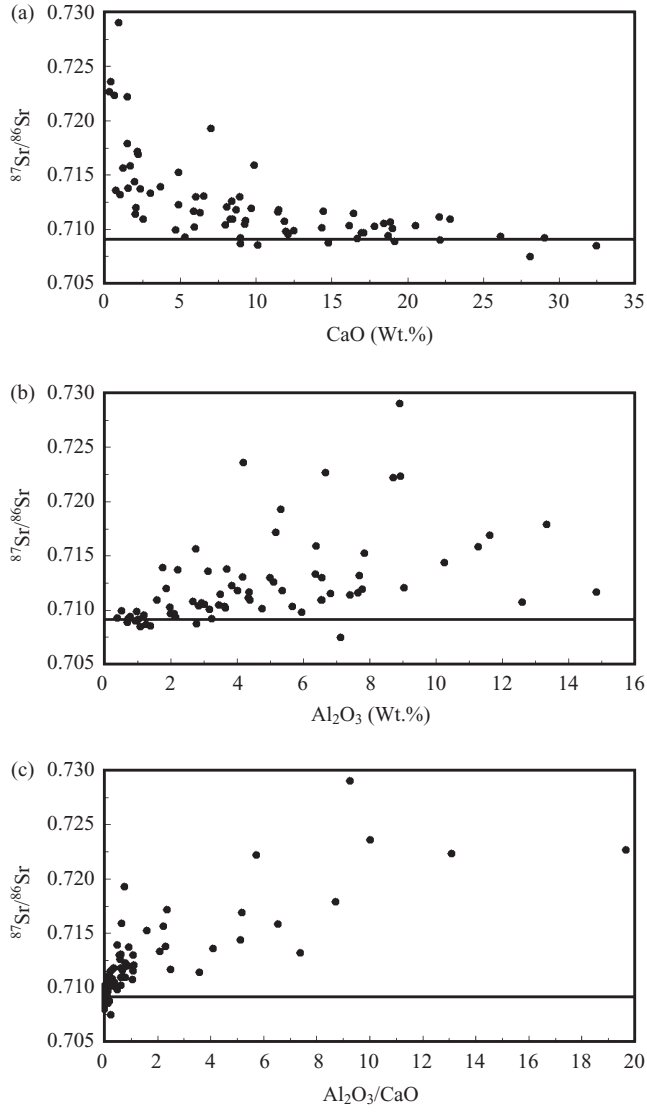

Figure 2 *(a) A plot of $^{87}Sr/^{86}Sr$ versus CaO. (b) A plot of $^{87}Sr/^{86}Sr$ versus Al_2O_3. (c) A plot of $^{87}Sr/^{86}Sr$ versus Al_2O_3/CaO. The horizontal lines represent the present-day seawater $^{87}Sr/^{86}Sr$ isotope ratio of 0.709165 (Stille and Shields 1997; Banner 2004).*

isotopic signature of IT34 to resemble that of seawater, while those of IT85 and IT87 would have to be a little lower. However, the results are somewhat different. Sands IT85 and IT34 have Sr isotopic signatures slightly above the modern value for seawater; that is, 0.71079 and 0.71034, respectively. The $^{87}Sr/^{86}Sr$ isotope ratio of sand IT87 is indeed lower than the seawater signature, at 0.70867. This is in accordance with its low Al_2O_3 content, which indicates that the contribution of radiogenic Sr from feldspar is very low. It therefore seems that (at least in the western Mediterranean; see below) the Sr isotopic signature is only indicative of the origin of the lime for

sands (and glass) with low concentrations of Al_2O_3, or better low Al_2O_3/CaO ratios. As a limit value for this Al_2O_3/CaO ratio, we can suggest 0.25 (e.g., for IT34 this value is 0.36, for IT85 0.29 and for IT87 0.14).

Twenty-four of the beach sands that were analysed for their Sr and Nd isotopic compositions contain insufficient calcareous fragments in order to provide sufficient CaO to produce a stable glass (see Brems *et al*. 2012a). These sands with CaO concentrations below 6% mostly have rather radiogenic Sr isotopic signatures (Fig. 2 (a)). The shortage of CaO in the sand could be compensated for by adding pieces of shell or limestone to the glass batch. By doing this, four of these lime-deficient sands (SP46, SP20, FR16 and IT01) could be used to produce glass with a composition very close to that of typical Roman natron glass (Brems *et al*. 2012a). Depending on the Sr content and Sr isotopic signature of the material added, this could result in a shift in the $^{87}Sr/^{86}Sr$ isotope ratios of the final glass as compared to the Sr isotopic signature of the sand. In order to determine the extent of this possible shift, we calculated the expected Sr concentrations and Sr isotopic signatures of the hypothetical natron glasses. This was done by using binary mixing equations (Faure and Mensing 2005). When two components with different Sr concentrations get mixed in varying proportions, the concentration of Sr in the resulting mixture is as follows:

$$Sr_M = Sr_A f_A + Sr_B(1 - f_A),$$

where Sr_M, Sr_A and Sr_B represent the Sr concentrations in the mixture, components A and B, respectively, and f_A and $(1 - f_A)$ express the fractions of component A and B, respectively. If these two components also have different isotopic signatures, the $^{87}Sr/^{86}Sr$ isotope ratio of the final mixture can be calculated using the following equation (Faure and Mensing 2005):

$$\left[\frac{^{87}Sr}{^{86}Sr}\right]_M = \frac{\left[\frac{^{87}Sr}{^{86}Sr}\right]_A f_A Sr_A + \left[\frac{^{87}Sr}{^{86}Sr}\right]_B (1 - f_A) Sr_B}{Sr_A f_A + Sr_B(1 - f_A)}.$$

For each lime-deficient sand, three calculations were performed, each one simulating glass production using a different source of additional lime. In the first calculation, the additional lime needed was assumed to come from shell material with a high Sr content of 4000 ppm and a $^{87}Sr/^{86}Sr$ isotope ratio equal to that of modern seawater: 0.709165 (Stille and Shields 1997; Banner 2004). For the second calculation, we used the Sr concentration and $^{87}Sr/^{86}Sr$ isotope ratio that was actually measured for shells collected from a number of beaches along the coasts of southern France and north-west Italy, as we would expect shells to have been collected by a local Roman glass producer. The shells were crushed, homogenized and analysed for their Sr concentration and $^{87}Sr/^{86}Sr$ isotope ratio in the same way as the beach sands. This resulted in a lower Sr concentration of 1568 ppm. The $^{87}Sr/^{86}Sr$ isotope ratio remained practically the same, at 0.70915. For the third calculation, we used theoretical limestone with a Sr content of 400 ppm and an $^{87}Sr/^{86}Sr$ ratio of 0.70750. The composition of the hypothetical glasses and the proportion of sand to additional lime was calculated as described by Brems *et al*. (2012a): the Na_2O and CaO levels were fixed at 16.63 and 7.48%, respectively (the average Na_2O and CaO content of Roman glass; Foster and Jackson 2009). We further assumed that the contribution of natron to the Sr budget of the glass is negligible.

The original Sr concentrations and $^{87}Sr/^{86}Sr$ isotope ratios of the lime-deficient sands and the calculated Sr contents and $^{87}Sr/^{86}Sr$ isotope ratios of the glasses are shown in Figure 3. Most of

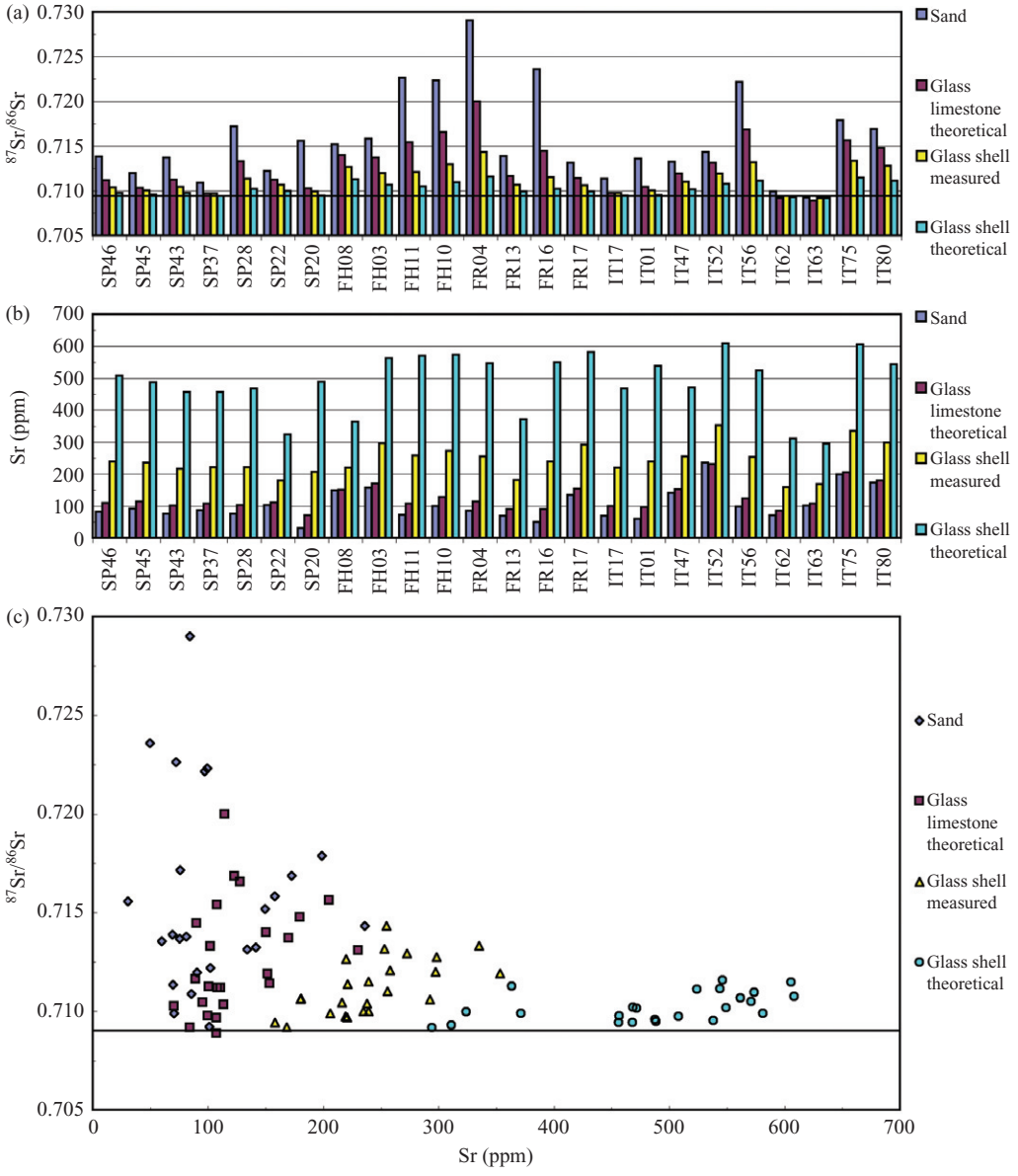

Figure 3 *(a) The $^{87}Sr/^{86}Sr$ isotope ratio of sands with insufficient CaO to produce Roman natron glass and the glass that can be produced from these sands after the addition of an extra source of lime (see text). (b) Sr concentrations. (c) A plot of $^{87}Sr/^{86}Sr$ versus the Sr concentration. The horizontal lines represent the present-day seawater $^{87}Sr/^{86}Sr$ isotope ratio of 0.709165 (Stille and Shields 1997; Banner 2004).*

the sands with low CaO concentrations initially have rather high and variable $^{87}Sr/^{86}Sr$ ratios (0.70922–0.72901) and relatively low Sr contents (30–236 ppm). After the addition of shell or limestone, the Sr isotopic signature of the resulting glass is shifted towards lower $^{87}Sr/^{86}Sr$ ratios (Fig. 3 (a)). The extent of this shift is strongly dependent on the concentration of Sr in

the source of additional lime. Shell with a high Sr content of 4000 ppm would have the largest influence. Glasses made with this kind of lime source would have $^{87}Sr/^{86}Sr$ isotope ratios between 0.70918 and 0.71158. For glasses made with the French and Italian seashells with a Sr concentration of 1568 ppm, the $^{87}Sr/^{86}Sr$ isotope ratio is less modified (0.70919–0.71433). The calculated $^{87}Sr/^{86}Sr$ isotope ratios of glasses produced with limestone are on average even higher and show a broader range (0.70889–0.71999), even though we used a low $^{87}Sr/^{86}Sr$ isotope ratio of 0.70750 for the limestone in the calculations. Only for one sample (IT63) is the final $^{87}Sr/^{86}Sr$ isotope ratio lower than the modern value for seawater. This sand already had a relatively low $^{87}Sr/^{86}Sr$ isotope ratio initially. It therefore seems that the Sr isotopic signature is not necessarily indicative of the source of lime in a glass. Our binary mixing calculations demonstrate that glass produced with Sr-rich seashell can still show a significant difference between its $^{87}Sr/^{86}Sr$ isotope ratio and that of seawater of up to 0.00241. Furthermore, we see that glass produced with these sands and limestone usually has higher $^{87}Sr/^{86}Sr$ ratios than those made with shell fragments.

The concentration of Sr in the calculated glasses is shown in Figures 3 (b) and 3 (c). It seems that the Sr concentration is more diagnostic for the source of lime. Glasses produced with shells with Sr contents of 4000 ppm would contain between 294 and 608 ppm Sr. Glasses made with limestone with 400 ppm Sr have Sr concentrations between 70 and 230 ppm. The range of Sr concentrations in glasses made with shell material with intermediate Sr contents, however, overlaps with both previous ranges. The use of the Sr content of glass as a provenance indicator of the lime source used thus seems to be limited by the wide possible range of Sr content in (partially recrystallized) aragonite and high-Mg calcite, from which the shells on modern beaches are made up.

AN EAST–WEST DISCREPANCY?

Freestone *et al*. (2003, and unpublished data) previously determined the Sr isotopic composition of raw glass from primary glass production sites in Egypt and Syro-Palestine, which were active between the fourth and eighth centuries AD. The Sr isotopic signature of the Levantine raw glass was found to be very close or slightly below the modern marine signature. Furthermore, they have high Sr contents between 300 and 500 ppm, suggesting the use of shell as source of lime. The Egyptian samples, however, had lower $^{87}Sr/^{86}Sr$ ratios and Sr contents between 100 and 200 ppm. These two observations support the idea of a limestone source of lime (Freestone *et al*. 2003). The same combination of seawater Sr isotopic signatures and high Sr concentrations, and low $^{87}Sr/^{86}Sr$ isotope ratios and low Sr contents, has been observed in numerous analyses of Roman natron glass (e.g., Wedepohl and Baumann 2000; Freestone *et al*. 2003; Degryse *et al*. 2006; Degryse and Schneider 2008). So why does this approach not seem to work for our calculated glasses? The problem seems to be that the Sr isotopic signature of the lime source is overshadowed by the influence of the Sr from the silicate fraction in the sands. In the western Mediterranean, Sr derived from the silicates is usually very radiogenic. However, lithogenic (i.e., non-carbonate) Nile sediments, which dominate the eastern Mediterranean, have lower $^{87}Sr/^{86}Sr$ ratios that are very close to, or lower than, the present-day value for seawater, with a pure Nile end-member of 0.707043 and sediments along the Nile Delta and the Levantine coast varying between 0.7075 and 0.7095 (Krom *et al*. 1999a,b; Weldeab *et al*. 2002). In the eastern Mediterranean, the influence of Sr from feldspar would thus be much smaller, and the final Sr isotopic signature of the glass would be left unaltered or only slightly lowered. Therefore we conclude that Sr isotopic signatures are indeed indicative of the source of lime for natron glass produced in the

eastern Mediterranean, whereas for glass made in the west this is not (always) the case. The Sr concentrations provide the same information in both regions.

CONCLUSIONS

With this study, we wanted to evaluate the use of Sr isotopic signatures for the provenance determination of Roman natron glass. Seventy-seven beach sands from Spain, France and Italy were analysed for their Sr isotopic compositions and, by using binary mixing equations, we were able to calculate the Sr isotopic signature of glass produced from these sands. The results of these calculations show that the addition of shell or limestone to the glass batch is often not enough to obscure the radiogenic Sr isotopic signature of the sand raw materials. Therefore, the $^{87}Sr/^{86}Sr$ isotope ratio of glass is not always indicative of the main source of lime. In this aspect, there seems to be a marked difference between the eastern and western Mediterranean. In the west, the silicate fraction of the sand often contains important amounts of radiogenic Sr, resulting in a shift in $^{87}Sr/^{86}Sr$ ratios to higher values. Since the Sr isotopic signatures of the Nile-dominated siliciclastic sediments in the eastern Mediterranean lie around or slightly below the modern-day seawater signature, the induced shift in the Sr isotopic signature of the glass is less explicit. For glasses produced in the eastern Mediterranean, the Sr isotopic signature is indeed a good provenance indicator for the source of lime. In the western part of the Mediterranean, this is only so for glasses with low Al_2O_3 concentrations and an Al_2O_3/CaO ratio lower than 0.25. The Sr content of the glass is a better and more robust indication of the lime source.

ACKNOWLEDGEMENTS

We are grateful to Steven Luypaers, Johan Honings and Elvira Vassilieva for their help with the sample preparation and ICP–OES analyses. This research is financially supported by the ERC Starting Grant ARCHGLASS Grant agreement no. 240750 and the FWO project no. 6.0864.09. Dieter Brems and Monica Ganio are currently working as Research Assistants at the Fund for Scientific Research—Flanders (FWO-Vlaanderen). Lieve Balcaen is a Senior Research Assistant at the Fund for Scientific Research—Flanders (FWO-Vlaanderen).

REFERENCES

Avanzinelli, R., Elliott, T., Tommasini, S., and Conticelli, S., 2008, Constraints on the genesis of potassium-rich Italian volcanic rocks from U/Th disequilibrium, *Journal of Petrology*, **49**, 195–223.

Banner, J. L., 2004, Radiogenic isotopes: systematics and applications to earth surface processes and chemical stratigraphy, *Earth Science Reviews*, **65**, 141–94.

Bentley, R. A., 2006, Strontium isotopes from the earth to the archaeological skeleton: a review, *Journal of Archaeological Method and Theory*, **13**, 135–87.

Brems, D., Degryse, P., Ganio, M., and Boyen, S., in press a, The production of Roman glass with western Mediterranean sand raw materials: preliminary results, *Glass Technology: European Journal of Glass Science and Technology A*.

Brems, D., Degryse, P., Hasendoncks, F., Gimeno, D., Silvestri, A., Vassilieva, E., Luypaers, S., Honings, J., 2012a, Western Mediterranean sand deposits as a raw material for Roman glass production, *Journal of Archaeological Science*, **39**, 2897–907.

Brems, D., Ganio, M., Latruwe, K., Balcaen, L., Carremans, M., Gimeno, D., Silvestri, A., Vanhaecke, F., Muchez, P., and Degryse, P., 2012b, Isotopes on the beach, part 2: neodymium isotopic analysis for the provenancing of Roman glass-making, *Archaeometry*, in press, doi: 10.1111/j.1475-4754.2012.00701.x.

Burke, W. H., Denison, R. E., Hetherington, E. A., Koepnick, R. B., Nelson, H. F., and Otto, J. B., 1982, Variation of seawater $^{87}Sr/^{86}Sr$ throughout Phanerozoic time, *Geology*, **10**, 516–19.

Conticelli, S., D'Antonio, M., Pinarelli, L., and Civetta, L., 2002, Source contamination and mantle heterogeneity in the genesis of Italian potassic and ultrapotassic volcanic rocks: Sr–Nd–Pb isotope data from Roman Province and southern Tuscany, *Mineralogy and Petrology*, **74**, 189–222.

De Muynck, D., Huelga-Suarez, G., Van Heghe, L., Degryse, P., and Vanhaecke, F., 2009, Systematic evaluation of a strontium-specific extraction chromatographic resin for obtaining a purified Sr fraction with quantitative recovery from complex and Ca-rich matrices, *Journal of Analytical Atomic Spectrometry*, **24**, 1498–510.

Degryse, P., and Schneider, J., 2008, Pliny the Elder and Sr–Nd isotopes: tracing the provenance of raw materials for Roman glass production, *Journal of Archaeological Science*, **35**, 1993–2000.

Degryse, P., Henderson, J., and Hodgins, G., 2009, Isotopes in vitreous materials, a state-of-the-art and perspectives, in *Isotopes in vitreous materials* (eds. P. Degryse, J. Henderson and G. Hodgins), 15–30, Studies in Archaeological Sciences, 1, Leuven University Press, Leuven.

Degryse, P., Schneider, J., Haack, U., Lauwers, V., Poblome, J., Waelkens, M., and Muchez, Ph., 2006, Evidence for glass 'recycling' using Pb and Sr isotopic ratios and Sr-mixing lines: the case of early Byzantine Sagalassos, *Journal of Archaeological Science*, **33**, 494–501.

Di Battistini, G., Montanini, A., Vernia, L., Venturelli, G., and Tonarini, S., 2001, Petrology of melilite-bearing rocks from the Montefiascone Volcanic Complex (Roman Magmatic Province): new insights into the ultrapotassic volcanism of central Italy, *Lithos*, **59**, 1–24.

Faure, G., and Mensing, T. M., 2005, *Isotopes: principles and applications*, 3rd edn, Wiley, New York.

Foster, H. E., and Jackson, C. M., 2009, The composition of 'naturally coloured' late Roman vessel glass from Britain and the implications for models of glass production and supply, *Journal of Archaeological Science*, **36**, 189–204.

Freestone, I. C., 2006, Glass production in Late Antiquity and the Early Islamic period: a geochemical perspective, in *Geomaterials in cultural heritage* (eds. M. Maggetti and B. Messiga), 201–16, Special Publications 257, Geological Society of London, London.

Freestone, I. C., 2008, Pliny on Roman glassmaking, in *Archaeology, history and science: integrating approaches to ancient materials* (eds. M. Matinón-Torres and Th. Rehren), 77–100, UCL Institute of Archaeology Publications, Oxford.

Freestone, I. C., Leslie, K. A., Thirlwall, M., and Gorin-Rosen, Y., 2003, Strontium isotopes in the investigation of early glass production: Byzantine and early Islamic glass from the Near East, *Archaeometry*, **45**, 19–32.

Graustein, W. C., 1989, $^{87}Sr/^{86}Sr$ ratios measure the sources and flow of strontium in terrestrial ecosystems, in *Stable isotopes in ecological research* (eds. P. W. Rundel, J. R. Ehleringer and K. A. Nagy), 491–512, Ecological Studies 68, Springer, New York.

Grousset, F. E., and Biscaye, P. E., 2005, Tracing dust sources and transport patterns using Sr, Nd and Pb isotopes, *Chemical Geology*, **222**, 149–67.

Hasendonckx, F., 2009, *Mineralogie en geochemie van Catalaanse zandafzettingen en hun gebruik als grondstof voor antieke glasproductie*, Unpublished master's thesis in geology, K.U. Leuven, Belgium.

Katz, A., Sass, E., Starinsky, A., and Holland, H. D., 1972, Strontium behavior in the aragonite–calcite transformation: an experimental study at 40–98°C, *Geochimica et Cosmochimica Acta*, **36**, 481–96.

Kinsman, D. J. J., 1969, Interpretation of Sr^{2+} concentrations in carbonate minerals and rocks, *Journal of Sedimentary Research*, **39**, 486–508.

Krom, M. D., Michard, A., Cliff, R. A., and Strohle, K., 1999a, Sources of sediment to the Ionian Sea and western Levantine basin of the eastern Mediterranean during S-1 sapropel times, *Marine Geology*, **160**, 45–61.

Krom, M. D., Cliff, R. A., Eijsink, L. M., Herut, B., and Chester, R., 1999b, The characterisation of Saharan dusts and Nile particulate matter in surface sediments from the Levantine basin using Sr isotopes, *Marine Geology*, **155**, 319–30.

Linn, A. M., and DePaolo, D. J., 1993, Provenance controls on the Nd–Sr–O isotopic composition of sandstones: examples from Late Mesozoic Great Valley forearc basin, California, in *Processes controlling the composition of clastic sediments* (eds. M. J. Johnson and A. Basu), 121–33, Geological Society of America Special Paper 284.

Rampone, E., Hofmann, A. W., and Raczek, I., 1998, Isotopic contrasts within the Internal Liguride ophiolite (N. Italy): the lack of a genetic mantle–crust link, *Earth and Planetary Science Letters*, **163**, 175–89.

Sayre, E. V., and Smith, R. V., 1961, Compositional categories of ancient glass, *Science*, **133**, 1824–6.

Shannon, R. D., 1976, Revised effective ionic radii and systematic studies of interatomic distances in halides and chalcogenides, *Acta Crystallographica*, **A32**, 751–67.

Shortland, A. J., 2004, Evaporites of the Wadi Natrun: seasonal and annual variation and its implication for ancient exploitation, *Archaeometry*, **46**, 497–516.

Shortland, A. J., Schachner, L., Freestone, I. C., and Tite, M., 2006, Natron as a flux in the early vitreous materials industry: sources, beginnings and reasons for decline, *Journal of Archaeological Science*, **33**, 521–30.

Silvestri, A., Molin, G., Salviulo, G., and Schievenin, R., 2006, Sand for Roman glass production: an experimental and philological study on source of supply, *Archaeometry*, **48**, 415–32.

Stanley, D. J., Krom, M. D., Cliff, R. A., and Woodward, J. C., 2003, Nile flow failure at the end of the Old Kingdom, Egypt: strontium isotopic and petrologic evidence, *Geoarchaeology*, **18**, 395–402.

Stille, P., and Shields, G., 1997, *Radiogenic isotope geochemistry of sedimentary and aquatic systems*, Lecture Notes in Earth Sciences 68, Springer-Verlag, Berlin.

Veizer, J., 1977, Diagenesis of pre-Quaternary carbonates as indicated by tracer studies, *Journal of Sedimentary Research*, **47**, 565–81.

Veizer, J., Ala, D., Azmy, K., Bruckschen, P., Buhl, D., Bruhn, F., Carden, G. A. F., Diener, A., Ebneth, S., Godderis, Y., Jasper, T., Korte, C., Pawellek, F., Podlaha, O. G., and Strauss, H., 1999, $^{87}Sr/^{86}Sr$, $\delta^{13}C$ and $\delta^{18}O$ evolution of Phanerozoic seawater, *Chemical Geology*, **161**, 59–88.

Wedepohl, K. H., 1978, Strontium, in *Handbook of geochemistry*, vol. II/4, section 38, Springer-Verlag, Berlin.

Wedepohl, K. H., 1995, The composition of the continental crust, *Geochimica et Cosmochimica Acta*, **59**, 1217–32.

Wedepohl, K. H., and Baumann, A., 2000, The use of marine molluskan shells for Roman glass and local raw glass production in the Eifel area (western Germany), *Naturwissenschaften*, **87**, 129–32.

Wedepohl, K. H., Simon, K., and Kronz, A., 2011a, Data on 61 chemical elements for the characterization of three major glass compositions in Late Antiquity and the Middle Ages, *Archaeometry*, **53**, 81–102.

Wedepohl, K. H., Simon, K., and Kronz, A., 2011b, The chemical composition including the rare earth elements of the three major glass types of Europe and the Orient used in Late Antiquity and the Middle Ages, *Chemie der Erde*, **71**, 289–96.

Weldeab, S., Emeis, K. C., Hemleben, C., and Siebel, W., 2002, Provenance of lithogenic surface sediments and pathways of riverine suspended matter in the eastern Mediterranean Sea: evidence from $^{143}Nd/^{144}Nd$ and $^{87}Sr/^{86}Sr$ ratios, *Chemical Geology*, **186**, 139–49.